

# MODELING THE DYNAMICS OF THE LAND-SEA BREEZE CIRCULATION FOR AIR QUALITY MODELING

MIKHAIL NOVITSKY<sup>1</sup>, DANNY D. REIBLE,<sup>2</sup> and BERNARDO M. CORRIPIO<sup>2</sup>

<sup>1</sup>*Institute of Experimental Meteorology, Obninsk, Soviet Union,* <sup>2</sup>*Department of Chemical Engineering, Louisiana State University, Baton Rouge, Louisiana 70803, U.S.A.*

(Received in final form 17 September, 1991)

**Abstract.** Conventional atmospheric dispersion and air quality models require that the wind field be known with a higher resolution than is currently available from field monitoring stations in most coastal areas. In this paper, a numerical model is developed to predict the wind flow field during the land-sea breeze. The form and assumptions and method of solution of the model are described. The model output is compared to atmospheric data taken from a field study conducted in the Santa Barbara Channel and Ventura-Oxnard plain in southern California.

## 1. Introduction

Air pollution as a result of industrial activities or mineral resource development (e.g., oil production) in a coastal area is controlled by the diurnal cycle of the land-sea breeze circulation. Differential heating between the water and land surfaces gives rise to a buoyancy-driven sea breeze directed onshore during the afternoon and a reverse land breeze during the night. The diurnal wind reversals can potentially limit the net ventilation of an air basin by recycling pollutants. Even during the land or sea breeze portion of the cycle, a balancing return flow aloft typically occurs that can retain pollutants within the coastal zone depending on the degree of interaction between the surface layer and the air aloft. In addition, surface heating of the land gives rise to a convective boundary layer that grows with distance from the shore. This can result in the fumigation of pollutants from aloft or increased interaction between the surface flow and the return flow. In order to assess the atmospheric pollution resulting from current or planned coastal development, the transport and dispersion of contaminants in this complex flow must be determined.

Conventional atmospheric dispersion and air quality models assume that the wind field is a known quantity. Often the wind field is not known with sufficient detail for state-of-the-art air quality simulation models and the available data are used to define the wind field by sophisticated interpolation techniques (e.g., Goodin *et al.*, 1979). Even this approach is often unsatisfactory in a coastal environment, however. The traditionally sparse wind monitoring network typically exists only over land, essentially limiting the known wind field to half of the domain of interest. In addition, the land-sea breeze is exceedingly complex with a sharply defined internal boundary layer (IBL) that varies significantly with both time and position. The dispersion of pollutants during the transition between

daytime and nighttime winds is particularly unclear. The wind reversals generally take place over a 1–3 h time period during which winds are light and variable, often below the threshold velocities of conventional anemometers. Despite this, contaminant dispersion during such a wind reversal can be very large (Reible, 1982).

To overcome the difficulty of the poor resolution of the recorded winds, it becomes necessary to predict the flow field in addition to contaminant transport and dispersion. It is necessary to be able to define the winds, the structure and depth of the IBL and the return flow aloft, and the spatial and temporal variation of the atmospheric mixing coefficients (e.g., turbulent diffusivities) in order to predict the contaminant behavior. The research described in this paper is directed toward development and testing of such a model of the land-sea breeze circulation.

## 2. Model Development

When choosing equations for the purpose of modeling the sea breeze circulations, we must have sufficiently high resolution to see the special character of the sea breeze regions. To simplify the analysis, however, let us consider only the two-dimensional case. Such a model is quite reasonable in that the curvature of the shoreline is often small and can be represented by a straight line. It should be recognized that hydrostatic approximations are inappropriate because the horizontal scale of the sea breeze front is of the same order as the vertical scale. In addition, let us seek a solution employing only first-order closure of the wind field using eddy diffusivity concepts. The coefficient of turbulent diffusivity must be calculated on the basis of the wind field and temperature. From these assumptions, we can write the following equations,

$$\begin{aligned}
 \frac{\partial u}{\partial t} + u \frac{\partial u}{\partial x} + w \frac{\partial u}{\partial z} &= -\frac{\partial \Phi}{\partial x} + fv - fV_g + k_x \frac{\partial^2 u}{\partial x^2} + \frac{\partial}{\partial z} k_z \frac{\partial u}{\partial z}, \\
 \frac{\partial v}{\partial t} + u \frac{\partial v}{\partial x} + w \frac{\partial v}{\partial z} &= fU_g - fu + k_x \frac{\partial^2 v}{\partial x^2} + \frac{\partial}{\partial z} k_z \frac{\partial v}{\partial z}, \\
 \frac{\partial w}{\partial t} + u \frac{\partial w}{\partial x} + w \frac{\partial w}{\partial z} &= -\frac{\partial \Phi}{\partial z} + g \frac{T'}{T_m} + k_x \frac{\partial^2 w}{\partial x^2} + \frac{\partial}{\partial z} k_z \frac{\partial w}{\partial z}, \\
 \frac{\partial T'}{\partial t} + u \frac{\partial T'}{\partial x} + w \frac{\partial T'}{\partial z} + wS &= k_x' \frac{\partial^2 T'}{\partial x^2} + \frac{\partial}{\partial z} \left\{ k_z' \left[ \frac{\partial T'}{\partial z} + S \right] \right\}, \quad (1) \\
 \frac{\partial u}{\partial x} + \frac{\partial w}{\partial z} &= 0,
 \end{aligned}$$

where  $u$ ,  $v$  and  $w$  are the mean components of the wind velocity in the  $x$ ,  $y$  and  $z$  coordinate directions. The  $x$ -axis is assumed to be directed perpendicular to the shore in the onshore direction while  $z$  represents the vertical coordinate.  $U_g$  and  $V_g$  represent the components of the geostrophic winds in the  $x$  and  $y$  directions;

$f = 1.03 \times 10^{-4} \text{ s}^{-1}$  is the Coriolis parameter;  $k_x$  and  $k_z$  are the horizontal and vertical components of the coefficient of turbulent diffusivity;  $k_x^t$  and  $k_z^t$  are the horizontal and vertical components of the coefficient of turbulent thermal diffusivity;  $S = \gamma_a - \gamma$  is a stability parameter, where  $\gamma_a$  is the adiabatic temperature gradient and  $\gamma$  is the mean background temperature gradient;  $T'$  is the deviation of temperature from the background mean temperature; and  $\phi = RT_m P'/P$ , where  $R$  is the ideal gas constant,  $T_m$  the mean temperature of air, and  $P'$  is the deviation of pressure from background mean pressure  $P$ .

Pressure, density and temperature in the above equations are written as sums of a mean component and a fluctuating component. The fluctuating components are a result of mesoscale variations in these quantities in the sea breeze circulation. It is presumed that the hydrostatic approximation applies to the background conditions:

$$\frac{1}{\rho} \frac{\partial P}{\partial z} + g = 0, \quad P = \rho RT, \quad \frac{\partial T}{\partial z} = -\gamma. \quad (2)$$

For determination of the coefficient of turbulent diffusion, the approach of Maddukuri (1982) was employed. This method is simple yet retains the key characteristics of observed turbulent diffusivity profiles. The following formulas were used to determine the vertical turbulent diffusion coefficient.

At the first four levels ( $z \leq 15 \text{ m}$ )

$$k_z = \begin{cases} \kappa u_* z \left(1 + 4.7 \frac{z}{L}\right)^{-1} & L \geq 0 \\ \kappa u_* z \left(1 - 15 \frac{z}{L}\right)^{1/14} & L < 0, \end{cases} \quad (3)$$

where  $u_*$  is friction velocity and  $L$  is the Monin-Obukhov length scale. For determination of  $u_*$  and  $L$ , we have used continuity of heat and momentum at the upper boundary of the surface layer (15 m).

For heights greater than 15 m but less than 50 m,

$$\begin{aligned} k_z &= l^2 S_w (1 + 3\text{Ri})^{-2} & \text{Ri} > 0, \\ k_z &= l^2 S_w (1 - 3\text{Ri})^2 & 0 \geq \text{Ri} \geq -0.048, \\ k_z &= 4.22 l^2 \left[ \frac{g}{\theta} \left| \frac{\partial \theta}{\partial z} \right| \right]^{1/2} & -0.048 > \text{Ri}, \end{aligned} \quad (4)$$

where  $\text{Ri}$  is the gradient Richardson number and  $\Theta$  is the potential temperature.  $S_w$  is defined by

$$S_w = \left\{ \left[ \frac{\partial u}{\partial z} \right]^2 + \left[ \frac{\partial v}{\partial z} \right]^2 \right\}^{1/2};$$

$l$  is a mixing length parameter given by Blackadar's formula  $l = \kappa z / (1 + \kappa z / l_\infty)$ , where  $l_\infty$  is the asymptotic mixing length.

For heights greater than 50 m,

$$\begin{aligned} k_z &= l^2 S_w (1 - 3\text{Ri}) & \text{Ri} \leq 0, \\ k_z &= l^2 S_w (1 + 3\text{Ri})^{-1} & \text{Ri} > 0. \end{aligned} \quad (5)$$

The coefficient of thermal conductivity is assumed proportional to the turbulent diffusivity:  $k'_z = \alpha_t k_z$ . The horizontal components of the turbulent heat and mass exchange coefficients are assumed constant at  $1000 \text{ m}^2/\text{s}$ .  $\alpha_t$ , the inverse of the turbulent Prandtl number, is assumed constant and equal to 1 under neutral or stable conditions and equal to 3 under unstable conditions.

The temperature on the underlying surface is a key parameter in Equations (1) since it drives the entire flow. Often when models are developed, surface temperature is calculated from surface energy balance. It is considered that a better way of estimation is use of near-surface temperature which is readily available from meteorological stations. This decision eliminates the necessity of solving the heat balance equation (a highly accurate solution is essential due to the strong dependence between onshore temperature and breeze circulation). The surface temperature  $T'(x, 0, t)$  is defined as

$$T'(x, 0, t) = \begin{cases} 0 & \text{above water,} \\ T_0(x, t) & \text{above land.} \end{cases}$$

$T_0(x, t)$  was measured at several sites and obtained at the grid points between them by linear interpolation.

The upper boundary condition matches the geostrophic background wind

$$u = U_g, \quad v = V_g, \quad w = 0, \quad T' = 0.$$

On the left and right boundaries of the region, homogeneous boundary conditions are assumed, i.e., all derivatives over  $x$  are equal to zero.

Surface roughness over land was an input parameter while surface roughness over water was calculated using the formula  $z_0 = 0.032 u_*^2 / g$  assuming that  $z_0 > 0.0015 \text{ cm}$ , where  $u_*$  is friction velocity (Pielke, 1974).

To nondimensionalize the equations, we shall use length scale  $L = A/S$  and time scale  $\tau = (T_m/gS)^{1/2}$ , where  $A$  is the maximum difference between soil and water temperatures. The length scale is of the order of the height of the convective layer. The time scale is of the order of the inverse of the Brunt-Vaisala frequency. One more length scale can be obtained from the input parameters by multiplying the velocity scale  $L/\tau$  by the lifetime of the sea breeze. This provides  $L_1 = (A/\Omega) g^{1/2} (T_m S)^{-1/2}$ , where  $\Omega$  is the Earth's angular velocity. Physically  $L_1$  is proportional to the horizontal scale of the breeze.

### 3. Method of Solution

In solving these equations, we use the method of Patrinos and Kistler (1977). The idea is as follows. On the first half step in time, the first, second and third equations from (1) are used to determine wind field components  $u^*$ ,  $v^*$ , and  $w^*$ , neglecting the pressure terms. The eddy diffusivity coefficients used in these calculations are those of the previous time steps. This velocity field does not, in general, satisfy the continuity equation. Therefore on the next step of the calculations, we must correct the pressure. On the second half step in time, we must solve the equations

$$\begin{aligned}\frac{\partial u}{\partial t} &= -\frac{\partial \phi}{\partial x}, \\ \frac{\partial w}{\partial t} &= -\frac{\partial \phi}{\partial z} + \frac{g}{T_m} T', \\ \frac{\partial u}{\partial x} + \frac{\partial w}{\partial z} &= 0.\end{aligned}\quad (6)$$

Substitution of the first two of these equations into the third one, i.e., into the continuity equation, provides a Poisson equation with a known right-hand side:

$$\frac{\partial^2 \phi}{\partial x^2} + \frac{\partial^2 \phi}{\partial z^2} = \frac{1}{\Delta t} \left[ \frac{\partial u^*}{\partial x} + \frac{\partial w^*}{\partial z} \right] + \frac{g}{T_m} \frac{\partial T'}{\partial z}, \quad (7)$$

where  $\Delta t$  is a time step. After solving Equation (7), we can find corrected values of the velocities by using Equations (6).

Let us now consider the fact that the second term on the right-hand side of Equation (7) is much larger than the first term. This can give rise to significant errors in the solution. As a remedy, Patrinos and Kistler (1977) proposed a decomposition of the pressure into a hydrostatic term and a dynamic term as  $\phi = \phi_s + \phi_d$ . The hydrostatic term is estimated from the hydrostatic equations:

$$\frac{\partial \phi_s}{\partial z} = \frac{g}{T_m} T'. \quad (8)$$

Equation (7) combined with Equation (8) gives for the dynamic pressure  $\phi_d$ :

$$\frac{\partial^2 \phi_d}{\partial x^2} + \frac{\partial^2 \phi_d}{\partial z^2} = \frac{1}{\Delta t} \left[ \frac{\partial u^*}{\partial x} + \frac{\partial w^*}{\partial z} \right] - \frac{\partial^2 \phi_s}{\partial x^2}. \quad (9)$$

After calculation of the wind speed, we find the field of temperature perturbations by solving the heat conduction equation and we can then calculate the field of eddy diffusivity coefficients.

Equations for the wind speed components and the temperature perturbations were solved using a decomposition method (Marchuk and Sarkisyan, 1988). The Poisson Equation (9) was solved by a direct method (Samarsky, 1978).

The numerical solution grid was chosen sufficiently large to encompass the entire

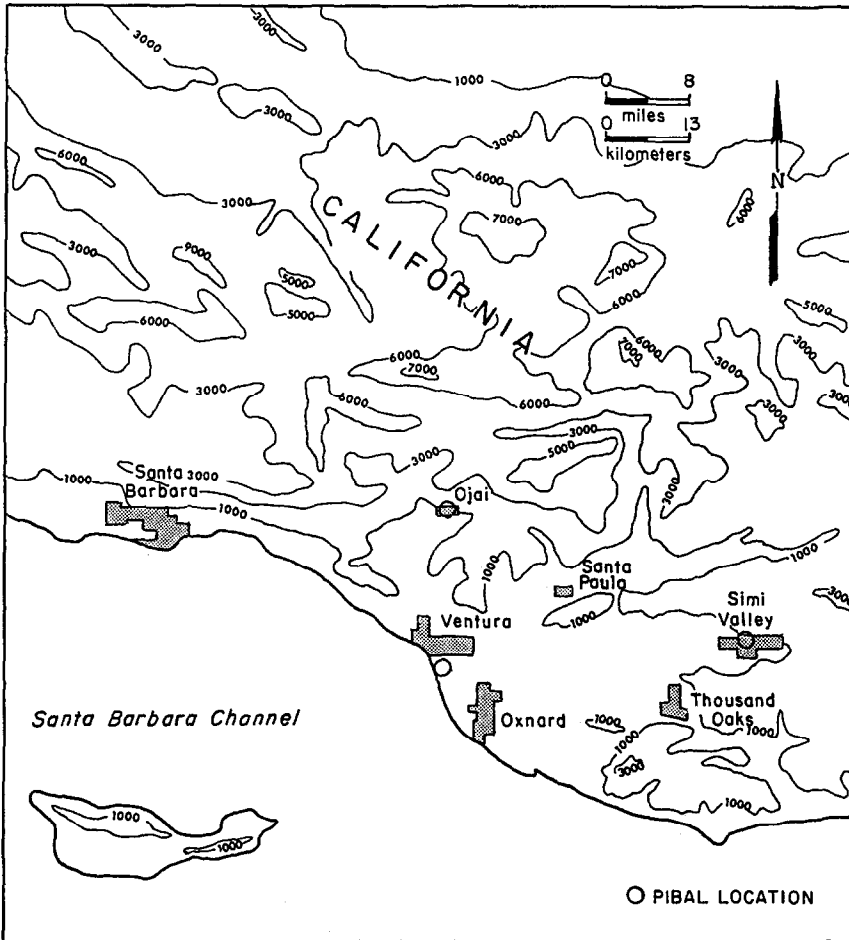


Fig. 1. Atmospheric dispersion study area: Santa Barbara Channel, Southern California.

region of the observed breeze circulation in the vicinity of the Ventura–Oxnard plain. The modeling domain was 3.4 km high and 128 km long. 35 nodal points in the vertical and 65 horizontal nodal points were used. The vertical grid was not taken to be homogeneous but instead the step size varied from 5 m near the surface to 150 m in the upper part of the region.

#### 4. The Meteorological Data Set

During the late summer and early fall of 1980, two separate atmospheric dispersion experiments were conducted in the Santa Barbara Channel of Southern California. The study area is shown in Figure 1. An atmospheric tracer, sulfur hexafluoride, was used to quantify atmospheric dispersion; and extensive meteorological measurements were made to assist in the interpretation of the collected data. These

meteorological measurements included surface and vertical profiles of wind speed, direction and temperature at selected onshore and offshore locations. As indicated in Figure 1, the analysis of the measured wind field is complicated by the complexity of the onshore terrain and by the curvature of the shoreline giving rise to a possibility of existence of a three-dimensional circulation. The Ventura–Oxnard portion of the study area, however, exhibits relatively flat and featureless terrain with an almost straight shoreline. Near-surface wind measurements over the plain also suggest that the sea breeze circulation is essentially two-dimensional with a measured mean afternoon wind direction throughout the plain of 215–255°. Thus the atmospheric tracer tests conducted in this region were considered to be valid for a comparison between model and experiment. The most complete meteorological data set was available for the period of September 28, including the preceding evening and subsequent morning. Thus this day was chosen for comparison.

The synoptic conditions were dominated by a ridge of high pressure at the surface and a weak low pressure trough located to the east (Lehrman *et al.*, 1981). The only apparent effect was that thermal lows were weaker in the interior region of California, well east of the test area. Skies were generally clear or had scattered clouds with unlimited ceilings and good visibility. The afternoon onshore breeze was quite consistent in both speed and direction and followed a clearly defined land breeze. The dimensionless potential temperature gradient aloft, i.e., the model stability parameter, varied from 0.004 to 0.008 °C/m both onshore and offshore throughout the period between 9/27/80 and the afternoon of 9/29/80. A radiosonde sounding of vertical temperature and relative humidity in the afternoon above a site approximately 7 km offshore, southwest of Ventura, is shown in Figure 2 (Schacher *et al.*, 1981). The stability parameter aloft based on this temperature profile is 0.007 °C/m, a value that was used in the model calculations.

The background wind conditions, or geostrophic winds, are less easily defined. Measured wind profiles over most of the region of interest did not extend sufficiently high to avoid some influence of the sea breeze or topographical influences. In addition, the winds aloft increased in the latter stages of the test at several sites presumably as a result of synoptic changes. As a result, the geostrophic background wind conditions were varied over the range of observed winds aloft until the predicted winds near the top of the computational grid agreed satisfactorily with the observed winds. The geostrophic winds were estimated in this manner to be about 1.5 m/s directed offshore. In the model coordinate system, the component perpendicular to the coast was determined to be about 1 m/s directed offshore and the component parallel to the coast was determined to be about 1 m/s directed toward the northwest. At Simi Valley, at the eastern end of the study region and presumably the least influenced by the sea breeze circulation, pilot balloon measurements during the early to mid-afternoon of 9/28 indicated the perpendicular component of the winds aloft (>2 km above ground level) to be between 1 and 2 m/s directed offshore. Ventura showed slightly higher winds aloft. The average perpendicular component from all wind measurements collected above

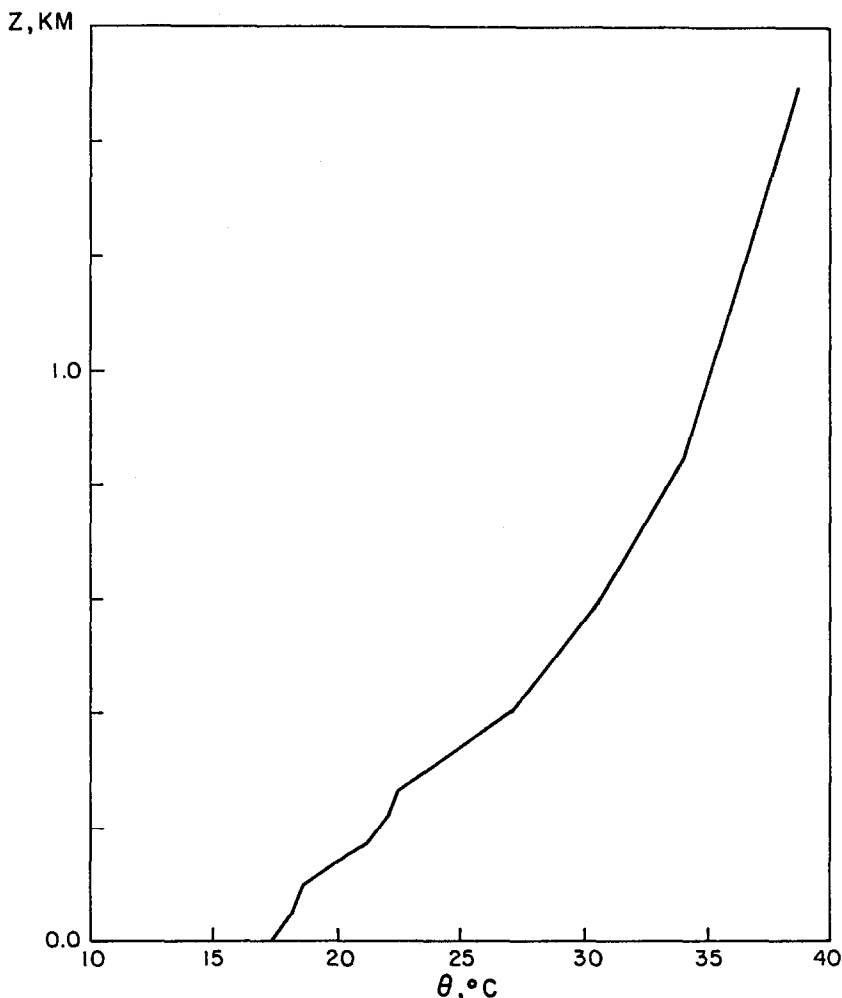


Fig. 2. Offshore potential temperature profile for dispersion study. From Schacher *et al.* (1981).

2 km was about  $-3$  m/s. The model results are relatively insensitive to the along-shore component and this component exhibited the most uncertainty.

The final parameter that must be specified is the temperature difference between air over land and water. The surface air temperature differences between Santa Paula and the location of the tracer release ship (7 km offshore) were used for this purpose. Santa Paula was the most centrally located of the Ventura–Oxnard monitoring sites. Sites closer to shore would presumably reflect the cooler temperatures over the water during the day. Sites farther from the coast were potentially influenced by the nearby mountain ranges, which formed the northern and eastern boundaries of the study area. The measured hourly temperature differences were



used in the model. The maximum temperature differences which occurred during the day between Santa Paula and the water surface was approximately  $10^{\circ}\text{C}$ .

## 5. Results

Calculations were made with the meteorological data described above. The starting time was the time of equal land and water surface temperatures (2000 Pacific Daylight Time (PDT), 9/27/80). The initial wind velocity profile was set to be an Ekman spiral. Temperature deviations from background were assumed to be zero throughout the domain. The results of an earlier study looking at the influence of input parameters on characteristics of the sea breeze circulation are reported in Novitsky (1988), who found that the flow characteristics are mostly affected by the background stability parameter and the surface temperature field as a function of time.

Analysis of the data for 9/28/80 shows that the breeze was non-frontal on that occasion: changes in wind direction occurred almost simultaneously at all observation points. A set of model runs under different conditions indicates that this was associated with the way in which the near-surface temperature varies as the onshore distance increases. According to the observations, the temperature in Santa Paula from 11 a.m. to 6 p.m. exceeded the temperature in Ventura by  $5\text{--}6^{\circ}\text{C}$ . If no dependence of onshore temperature on distance from the coast is assumed, the model predicts that the sea breeze circulation is frontal in character. But if linear growth of temperature is specified from the shoreline to Santa-Paula, a non-frontal sea breeze is predicted with an essentially simultaneous wind velocity change at different distances from shore. The calculations also show that the time dependence of wind velocity will fit measurement data only if the time dependence of near-surface temperature is taken from observations. When time variations of near-surface temperature are set, as in the earlier work (Novitsky, 1988), major phase errors appear.

The calculated wind field is shown in Figure 3 for 1500 PDT. The onshore-directed sea breeze in the lower layers is evident as is the balancing offshore-directed winds aloft. The convergence near the landward extent of the sea breeze is marked by updrafts. The resolution of the measured wind field is insufficient to compare the complicated flow predicted in this region to the atmospheric observations but the basic character of the observed sea breeze layer was reproduced by the model predictions. The detailed structure of the sea breeze front is sensitive to the horizontal effective diffusivity used in the model. The flow behind the front, however, was not a strong function of the horizontal effective diffusivity.

Figure 4 compares calculated and measured profiles of wind velocity. Shown are  $u$ -components for onshore and offshore flow at Ventura, Ojai and Simi Valley at three times. The discrepancy is greater for upper parts of the profiles where errors in estimating geostrophic conditions or synoptic-scale pressure variations

FIGURE 3. PREDICTED WIND FIELD

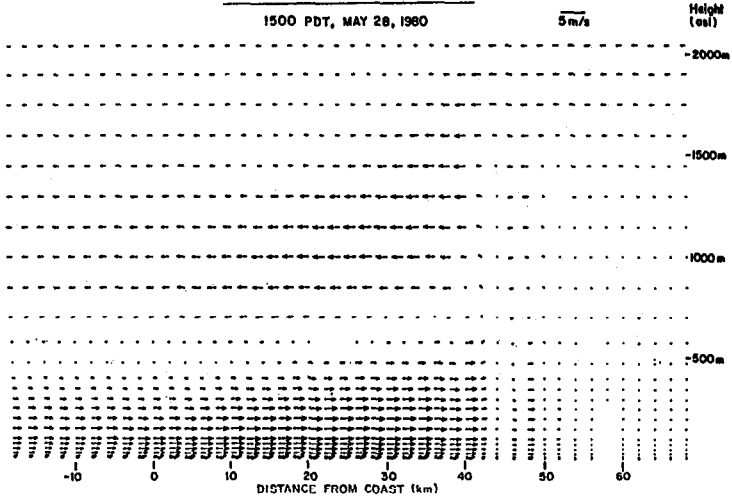


Fig. 3. Vector representation of the sea breeze wind field predicted at 1500 PDT, September 28, 1980.

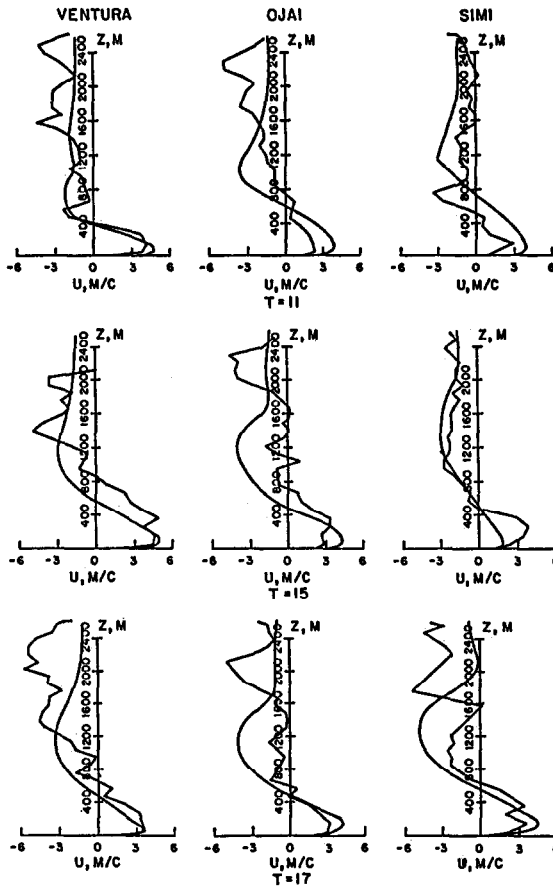


FIGURE 4. CALCULATED AND MEASURED HORIZONTAL WIND VELOCITY PROFILES DURING SEA BREEZE

Fig. 4. Calculated and measured horizontal wind velocity profiles during a sea breeze.

TABLE I

Comparison of model predictions and measured values for surface-layer depth and maximum surface and return velocities.

Location:		Ventura		Ojai		Simi	
Time:		Expt.	Model	Expt.	Model	Expt.	Model
1100	Surface-Layer Depth (m)	400	380	780	610	510	750
	Max. Surface Velocity (m/s)	4.2	4.8	2.4	3.9	3.0	4.0
	Max. return Velocity (m/s)	-4.3	-2.2	-4.9	-3.7	-3.3	-3.1
1500	Surface-Layer Depth (m)	870	580	710	390	480	530
	Max. Surface Velocity (m/s)	5.0	5.1	3.3	4.4	3.9	1.9
	Max. Return Velocity (m/s)	-5.0	-3.1	-4.7	-4.0	-2.8	-3.1
1700	Surface-Layer Depth (m)	670	480	470	490	630	550
	Max. Surface Velocity (m/s)	3.8	3.5	3.2	4.4	3.6	4.5
	Max. Return Velocity (m/s)	-5.8	-3.5	-5.1	-4.2	-5.3	-4.9

are most evident. Table I compares calculated and measured maximum surface and recirculation velocities and surface-layer height (defined as the height at which the velocity first becomes negative). The model predicts surface velocity well except at Simi, where the sea breeze is enhanced by the upslope breeze on neighboring mountains. The return velocity is modeled less well due to the inability to match geostrophic conditions and synoptic-scale pressure variations. The agreement in surface-layer depth appears satisfactory once it is recognized that the experimental measurements have a precision of  $\pm 100$  m.

A good indicator of the quality of the model is its ability to simulate the behavior of wind-turning angle with height. Figure 5 shows the height dependence of the calculated and measured wind-turning angles for Ventura. The discrepancy increases with height as was the case with longitudinal components of wind velocity.

The ability of the model in question to simulate spatial and temporal changes of mixing-layer height is considered by Novitsky (1988). The asymptotic mixing length,  $l_{\infty}$ , was selected to ensure agreement between calculated and observed results. The best fit with experimental data was obtained at  $l_{\infty}$  in the range of 25–50 m. At the same time, calculation of turbulent characteristics from local derivatives during convective conditions does not yield good results: in a properly mixed layer, the gradients are close to zero, yet intense mixing takes place in the layer. The  $\alpha_1$  value for such conditions is also not known well enough. We had to

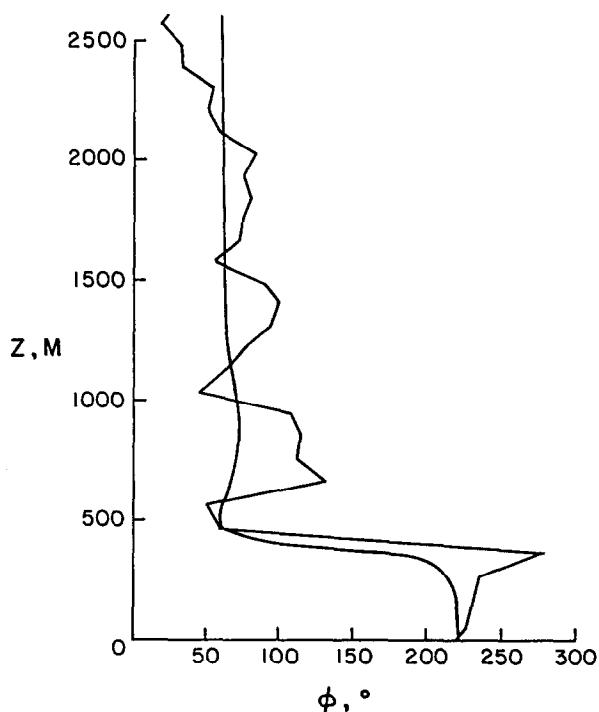


Fig. 5. Height dependence of calculated and measured wind-turning angles at Ventura.

calibrate for this value and assumed  $\alpha_t = 3$  which was reasonable for unstable conditions. It was assumed that  $\alpha_t = 1$  under stable conditions. On subsequent model versions, more advanced approaches are planned for calculating turbulence characteristics.

## 6. Conclusions

This paper describes a 2-dimensional non-hydrostatic mesoscale model which was used for modeling the land-sea breeze circulation in the Santa Barbara Channel in Southern California. The model gives a good description of spatial-temporal characteristics of the flow. A thorough account of the basic physical features of the sea breeze circulation in the model enabled realistic results as compared to observations. Thus, the model has been shown to be suitable for reconstructing profiles of meteorological values when calculating pollutant dispersion by a sea breeze.

Based on the generally encouraging results obtained, current research is directed toward modeling contaminant transport using the generated flow field. In addition, the model is being used to evaluate a laboratory facility capable of simulating the land-sea breeze circulation. The results of this latter research will be presented in another paper.

### Acknowledgements

This study has been performed in the framework of the Intergovernmental Soviet-American Agreement on Cooperation in Environmental Protection, Project 02.03-31. Dr. Novitsky is the Project Director for the USSR. We thank George Baughman and Chuck Steen, Past and Current Project Directors for the U.S.

### References

- Goodin, W. R., McRae, G. J., and Seinfeld, J. H.: 1979, 'A Comparison of Interpolation Methods for Sparse Data: Application to Wind and Concentration Fields', *J. Appl. Meteorol.* **18**, 761-771.
- Lehrman, D. E., Smith, T. B., Reible, D. D., and Shair, F. H.: 1981, 'A Study of Transport into Within and Out of Coastal Areas of Southern Santa Barbara County and Ventura County', MR-81-FR-1808, Final Report to Ventura Air Pollution Control District.
- Maddukuri, C. S.: 1982, 'A Numerical Simulation of an Observed Lake Breeze over Southern Lake Ontario', *Boundary-Layer Meteorol.* **23**, 369-387.
- Marchuk, G. I. and Sarkisyan, A. S.: 1988, *Mathematical Modeling of Ocean Circulation*, Springer-Verlag, Berlin, 292 pp.
- Novitsky, M. A.: 1988, 'Modeling the Influence of the Synoptic Wind on the Sea Breeze Circulation', *Meteorology and Hydrology* **7**, 74-81 (in Russian).
- Patrinos, A. A. N. and Kistler, A. L.: 1977, 'A Numerical Study of the Chicago Lake Breeze', *Boundary-Layer Meteorol.* **12**, 93-123.
- Pielke, R.: 1974, 'A Three-Dimensional Model of the Sea Breeze over South Florida', *Monthly Weather Rev.* **102**, 115-139.
- Reible, D. D.: 1982, 'Investigation of Complex Atmospheric Flow System', Ph.D. Dissertation, California Institute of Technology, Pasadena, 360 pp.
- Samarsky, A. A. and Nikolaev, E. S.: 1978, *Methods of Solving Grid Equations*, Nauka, Moscow (in Russian).
- Schacher, G. E., Davidson, K. L., Leonard, C. A., Spiel, D. E., and Fairull, C. W.: 1981, 'Offshore Transport and Diffusion in the Los Angeles Bight-1', NPS Data Summary, Report NSP-61-81-004, Naval Postgraduate School, Monterey, California.